Double Vectors Model Predictive Torque Control Without Weighting Factor Based on Voltage Tracking Error

Xiaoguang Zhang, *Member, IEEE*, and Benshuai Hou

***Abstract*—In order to reduce the computation burden and eliminate the weighting factor in conventional model predictive torque control (MPTC), this paper proposes an improved MPTC algorithm without the use of weighting factor. Based on the deadbeat direct torque and flux control, the reference voltage vector, which would be applied in the next period, is predicted to avoid testing all feasible voltage vectors, hence reducing the computation burden of conventional MPTC. Moreover, the torque and flux error-based cost function of conventional MPTC is replaced by the voltage vector tracking error-based cost function; thus, the weighting factor of stator flux in conventional MPTC, which is always necessary because of the different units between torque and flux, is eliminated. Furthermore, two voltage vectors, which include an active vector and a null vector, are applied during one control period to improve steady-state performance. The durations of the selected voltage vectors are determined based on the principle of voltage vector tracking error minimization. Moreover, to further improve the steady-state performance, a different vector selection way, in which the second voltage vector is not fixed as a null vector but selected in a border range, is introduced. The selection process of candidate voltage vectors is analyzed, and the duration is calculated. Simulation and experimental results both show the validity of the proposed control approach.**

***Index Terms*—Model predictive torque control (MPTC), permanent-magnet synchronous motor (PMSM), two vectors, weighting factor.**

I. Introduction

DIGITAL control systems of a permanent-magnet synchronous machine (PMSM) are now widely used in industrial applications, due to their high precision, high efficiency, and excellent control performance. In a practical PMSM system, quick dynamic response is the key factor that decides the performance of the whole system. Thus, to improve the dynamic performance of control system, model predictive torque control (MPTC) is recently introduced into the application of high performance dynamic control of PMSM drives [1]–[8]. In the MPTC method, the future states of system are predicted based on inherent discrete nature of motor inverter. Then, the cost function that is usually composed of the errors of predictive state (such as torque and stator flux in motor drives) is designed to determine the best voltage vector applied in next control period.

In conventional MPTC, to achieve simultaneous control of torque and stator flux, the cost function usually is designed based on torque and stator flux errors. However, the torque and stator flux have different unit and dimension; a suitable weighting factor in cost function is required to balance control performance between torque and stator flux. But it is an uphill task to tune the weighting factor because of the lack of theoretical design procedure. In order to solve this problem, the weighting factor design method based on the principle of torque ripple minimization is presented in [9]. To obtain a proper weighting factor, literature [10] proposes a fuzzy decision-making strategy. Other solutions include multiobjective ranking-based method [11], empirical procedure approach [12], and so on. Although aforementioned methods have been proved that they are effective, the complicated design step affects their further application in the practical system.

Apart from the tuning task of weighting factor, other challenges in MPTC, such as high torque ripple and high computation burden, also need to be faced [13]. In [22] and [23], two-vector-based model predictive power control strategies for ac/dc converter have been proposed, which effectively improve the steady-state control performance of system. Recently, to improve torque control performance, a two-vector-based MPTC strategy also has been reported [9], [13]. In this strategy, the optimal nonzero voltage vector is first selected from six active vectors according to the cost function minimization, and its duration is subsequently calculated based on some principles, then, the rest time of one control period is allocated for a null vector. It means that the voltage vector applied in next control period consists of two parts, i.e., a nonzero vector and a null vector. Although, a two-vector-based MPTC strategy can achieve better control performance, the computation burden increases.

Manuscript received November 21, 2016; revised February 7, 2017; accepted March 31, 2017. Date of publication April 6, 2017; date of current version December 1, 2017. This work was supported in part by the National Natural Science Foundation of China under Grant 51507004, in part by Beijing Natural Science Foundation under Grant 3172011, and in part by the Outstanding Young Scholars Fund of North China University of Technology under Grant XN018027. Recommended for publication by Associate Editor W. Qiao. *(Corresponding author: Xiaoguang Zhang.)*

The authors are with the Inverter Technologies Engineering Research Center of Beijing, North China University of Technology, Beijing 100144, China, the Collaborative Innovation Center of Key Power Energy-Saving Technologies, Beijing 100144, China, and also with the Collaborative Innovation Center of Electric Vehicles, Beijing 100144, China (e-mail: zxg@ncut.edu.cn; junhuige@163.com).

Color versions of one or more of the figures in this paper are available online at http://ieeexplore.ieee.org.

Digital Object Identifier 10.1109/TPEL.2017.2691776

In particular, for multistep prediction or for the application of multilevel converter, the computational burden rises exponentially [14], [15]. Therefore, to reduce the computation time, some methods have been proposed, such as sphere decoding algorithm [16], [17], the binary search tree method [18], and multiparametric toolbox-based multiparametric programming method [19]. Unfortunately, it is difficult to use these methods to reduce computation time online because of lack of real-time optimization capability.

In order to reduce the computation time and avoid the tedious tuning work of weighting factor in conventional MPTC, a reference voltage vector-based MPTC is proposed in this paper. The solution of DB-DTFC is adopted to obtain the expected voltage vector. This expected vector is used as reference vector of all feasible voltage vectors to determinate the optimal voltage vector, which reduces the number of candidate voltage vectors from six to one. Hence, computation burden of MPTC is significantly reduced. Then, a novel cost function, which is based on the error between reference voltage vector and candidate voltage vector, is proposed to select the optimal voltage vector. The torque and flux error-based cost function in conventional MPTC is replaced, then, the weighting factor in conventional MPTC, which is always necessary because of the different units between torque and flux, is eliminated. Moreover, to achieve better control performance, a null vector is introduced into selected optimal vector. It means that two voltage vectors that include an active vector and a null vector are applied during one control period. The durations of nonzero vector and null vector are determined based on the principle of voltage vector tracking error minimization. Furthermore, to further improve the steady-state performance of proposed MPTC, the second voltage vector is not fixed as a null vector but selected in a border range. The selection process of candidate voltage vectors is analyzed, and the duration is calculated. Simulation and experimental results both show the validity of the proposed method.

II. PMSM Model

Assuming that the employed PMSM has negligible cross-coupling magnetic saturation, structural asymmetry, iron losses, magnet eddy current loss, and harmonics in the descriptive functions of windings, rotor anisotropy, and coercive force of magnets, the model of surface-mounted permanent-magnet synchronous motor (SPMSM) in synchronous rotating frame can be described as follows [21]:

$$\begin{cases} u_d = R_s i_d - \omega\psi_q + \dfrac{d\psi_d}{dt} \\ u_q = R_s i_q + \omega\psi_d + \dfrac{d\psi_q}{dt} \end{cases} \tag{1}$$

$$\begin{cases} \psi_d = L_d i_d + \psi_f \\ \psi_q = L_q i_q \end{cases} \tag{2}$$

$$T_e = \frac{3}{2} p \psi_f i_q. \tag{3}$$

In this model, u_d and u_q are d- and q-axes stator voltages, i_d and i_q are d- and q-axes currents, ψ_d and ψ_q are d- and q-axes flux linkage, $L_d = L_q = L_s$ is stator inductance, R_s is winding resistance, ψ_f is flux linkage of permanent magnets, and ω is angular velocity (rad/s).

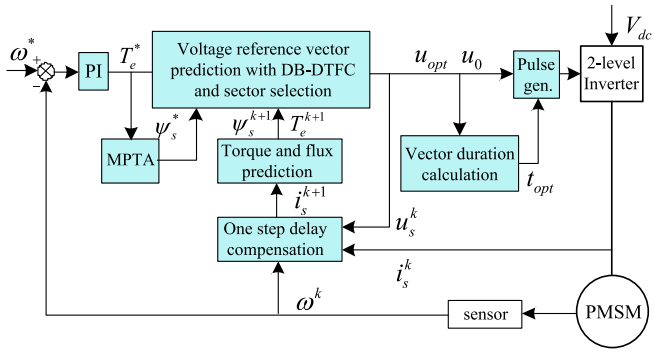

Fig. 1. Control diagram of the proposed MPTC method.

III. Double-Vectors MPTC Method (DVMPTC) With One Nonzero Vector and One Null Vector

The control program of the DVMPTC method with one nonzero vector and one null vector is shown in Fig. 1, which mainly includes the following parts: voltage reference vector prediction with DB-DTFC and sector selection, torque and flux prediction, delay compensation, and vector duration calculation. In addition, the torque reference T_e^* is obtained by the output of speed PI regulator, and the flux reference ψ_s^* can be calculated by the MPTA algorithm based on the torque reference [20]. The details of this method will be elaborated in the following text.

A. One Step Delay Compensation

In digital implementation, one step delay between selected voltage vectors and applied voltage vectors exists, because the selected voltage vector at current control period would be applied until next control period [24]. This delay degrades the control performance of system, especially for the system with low switching frequency. Therefore, to reduce the negative impact on control performance, delay compensation is quite necessary. The details of control delay compensation are elaborated in the following text.

Substituting (2) into (1), the voltage equation can be rewritten as follows:

$$L_s \frac{di_s}{dt} = u_s - R_s i_s - j\omega\psi_f e^{j\theta}. \tag{4}$$

Based on Euler-forward discretization method, the prediction of the stator current at next control period can be obtained, as shown in (5). Then, predictive current ${i_s}^{k+1}$ is used for replacing the sampled current i_s^k to compensate one-step delay

$$i_s^{k+1} = i_s^k + \frac{T_s}{L_s}\left(u_s^k - R_s i_s^k - j\omega\psi_f e^{j\theta}\right) \tag{5}$$

where T_s represents sampling period.

Although Euler-forward based (5) is simple and relatively easy to implement, its prediction precision is not high. Then, based on (5), a second-order Euler discretization method, which includes two parts, i.e., forward Euler integration and

trapezoidal integration, is adopted to improve prediction accuracy. Its discrete expression is given by

$$\begin{cases} i_p^{k+1} = i_s^k + \dfrac{T_s}{L_s}\left(u_s^k - R_s i_s^k - j\omega\psi_f e^{j\theta}\right) \\ i_s^{k+1} = i_p^{k+1} + \dfrac{T_s R_s}{2L_s}\left(i_p^{k+1} - i_s^k\right) \end{cases} \tag{6}$$

where i_s^{k+1} is predictive value of current, and i_p^{k+1} is predictor-corrector of current. The first equation of (6) is forward Euler integration part, which is considered as a rough approximation of i_s^{k+1}. The second equation of (6) is equivalent to the trapezoidal integration method, in which the i_p^{k+1} is used as the initial value.

B. DB-DTFC-Based Reference Voltage Prediction

In this paper, the solution of DB-DTFC is adopted to obtain the expected voltage vector. This expected voltage vector is used as reference vector of all feasible voltage vectors to determinate the candidate voltage vector. The details of this procedure will be elaborated in the following text.

In order to compensate the control delay, the predictive currents based on (6) are used to replace the measured currents of model (1), (2) and (3). Then, based on delay compensated voltage equation (1) and flux equation (2), the following equation can be obtained:

$$\begin{cases} \psi_d^{k+2} = u_d^{k+1}T_s + \psi_d^{k+1} + \omega T_s\psi_q^{k+1} - \dfrac{R_s T_s}{L_d}\left(\psi_d^{k+1} - \psi_f\right) \\ \psi_q^{k+2} = u_q^{k+1}T_s + \psi_q^{k+1} - \omega T_s\psi_d^{k+1} - \dfrac{R_s T_s}{L_q}\psi_q^{k+1}. \end{cases} \tag{7}$$

Next, substituting q-axis flux equation (2) into torque equation (3) yields

$$T_e = \frac{3}{2}p\psi_f\frac{\psi_q}{L_s}. \tag{8}$$

Taking the time derivative of the torque yields

$$T_e^{k+2} - T_e^{k+1} = \frac{3}{2}p\frac{\psi_f}{L_s}\left(\psi_q^{k+2} - \psi_q^{k+1}\right). \tag{9}$$

Then, substituting (7) into (9), the discrete state equation of torque for SPMSM can be expressed as follows:

$$T_e^{k+2} - T_e^{k+1} = \frac{3p\psi_f}{2L_s}\left(u_q^{k+1}T_s - \frac{R_s T_s\psi_q^{k+1}}{L_s} - \omega T_s\psi_d^{k+1}\right). \tag{10}$$

In addition, since voltage drop of resistance is much smaller than stator voltage when motor operates stably, item of resistance in (7) can be ignored. Then, the stator flux and voltage can be described as follows:

$$\begin{aligned} \left(\psi_s^{k+2}\right)^2 &= \left(\psi_d^{k+2}\right)^2 + \left(\psi_q^{k+2}\right)^2 \\ &= \left(u_d^{k+1}T_s + \psi_d^{k+1} + \omega T_s\psi_q^{k+1}\right)^2 \\ &\quad + \left(u_q^{k+1}T_s + \psi_q^{k+1} - \omega T_s\psi_d^{k+1}\right)^2. \end{aligned} \tag{11}$$

Based on the principle of deadbeat control, in order to obtain desired torque and stator flux response in next control period, the torque and stator flux (T_e^{k+2} and ψ_s^{k+2}) should be selected as reference values, which means $T_e^{k+2} = T_e^*$ and $\psi_s^{k+2} = \psi_s^*$. Thus, according to (10) and (11), the solution of DB-DTFC, which is called reference voltage vector in this paper, can be obtained as follows:

$$\begin{cases} u_d^{k+1} = \dfrac{-X_1 \pm \sqrt{X_1^2 - X_2}}{T_s} \\ u_q^{k+1} = \dfrac{B}{T_s} \end{cases} \tag{12}$$

where

$$\begin{aligned} X_1 &= \psi_q^{k+1} + \omega\psi_q^{k+1}T_s \\ X_2 &= B^2 + 2B(\psi_q^{k+1} - \omega\psi_d^{k+1}T_s) + \left(\psi_d^{k+1}\right)^2 + \left(\psi_q^{k+1}\right)^2 \\ &\quad + \omega^2 T_s^2\left[\left(\psi_d^{k+1}\right)^2 + \left(\psi_q^{k+1}\right)^2\right] - \left(\psi_s^*\right)^2 \\ B &= \frac{2L_q}{3p\psi_f}(T_e^* - T_e^{k+1}) + \frac{R_s T_s\psi_q^{k+1}}{L_q} + \omega T_s\psi_d^{k+1}. \end{aligned}$$

The phase angle can be easily obtained by transforming reference voltage vector (12) to the $\alpha\beta$ frame. The transformation expression is given by

$$u_{\mathrm{ref}} = \begin{pmatrix} {u_\alpha}^{k+1} \\ {u_\beta}^{k+1} \end{pmatrix} = \begin{pmatrix} \cos\theta & -\sin\theta \\ \sin\theta & \cos\theta \end{pmatrix}\begin{pmatrix} u_d^{k+1} \\ u_q^{k+1} \end{pmatrix}. \tag{13}$$

Then, the angle θ_{ref} of reference voltage vector can be obtained by

$$\theta_{\mathrm{ref}} = \arctan\left(\frac{u_\beta^{k+1}}{u_\alpha^{k+1}}\right). \tag{14}$$

C. Cost Function Design

In conventional MPTC, stator flux and torque error-based cost function shown in (15) is usually used as the criterion to select the optimal voltage vector

$$g = \left|T_e^* - T_e^{k+1}\right| + A\left|\psi_s^* - \left|\psi_s^{k+1}\right|\right| \tag{15}$$

where *A* is the weighting factor. In general, the weighting factor can be selected based on the principle of equal importance between torque and stator flux, which means that the weighting factor *A* satisfies $A = T_N/|\psi_{sN}|$. T_N is rated torque and ψ_{sN} is rated stator flux. However, in practical application, selected weighting factor based on (15) cannot obtain satisfied control performance. Thus, lots of work is required to tune the value of weighting factor by simulation or experiment.

In conventional MPTC, system discrete model and inherent discrete nature of motor inverter are adopted to predict the future behavior of states and determines the optimal voltage vector applied in the future by minimizing cost function (15). In other words, the main purpose of the conventional MPTC is to obtain a proper voltage vector to minimize the errors of torque and stator flux. However, in the proposed MPTC method, the reference vector of this proper voltage vector can be obtained by DB-DTFC solution (13), the reference voltage vector can ensure the errors of torque and stator flux converge to zero in one control period according to the principle of DB-DTFC. Thus, the only

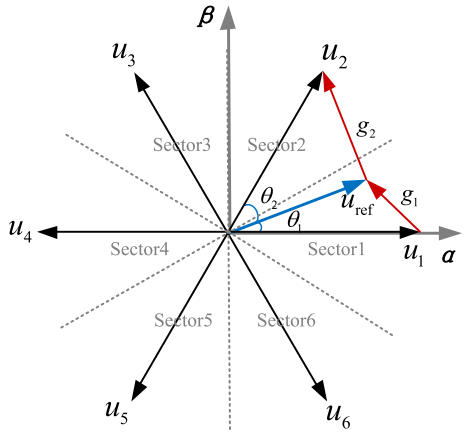

Fig. 2. Principle diagram of first vector selection.

work in this paper is to select a voltage vector closest to the reference vector. Therefore, a novel cost function is proposed to select the optimal voltage vector. Its expression is shown as follows:

$$g = |u_{\text{ref}} - u_i| \tag{16}$$

where u_{ref} is reference voltage vector, and u_i represents candidate voltage vectors. It is evident that in this novel cost function, the weighting factor is no longer required since only the tracking error of voltage vector is involved.

The core idea of the proposed method is consistent with the conventional method, but the realization modes are different. Conventional cost function adopts indirect voltage selection mode to obtain optimal voltage vector. However, the proposed cost function directly compares the reference voltage vector and candidate voltage vector to select optimal one, it is a kind of direct voltage selection mode.

D. Vector Selection and Duration Calculation

In this method, one control period is divided into two parts, one for the nonzero vector and the rest of time for a null vector. Thus, the key task is to select the first voltage vector from six nonzero vectors. In order to intuitively select first voltage vector, the whole $\alpha\beta$ plane is divided into six sectors, which is shown in Fig. 2. Each sector consists of one nonzero vector. According to the phase angle (14) of reference voltage vector, the sector position of reference voltage vector is able to be located. Then, first voltage vector can be determined. For example, if reference voltage vector (u_{ref}) is located in sector 1, as shown in Fig. 2, voltage vector u_1 should be selected as optimal vector, which means that u_1 can minimize the cost function g.

In order to prove that u_1 is the optimal vector, u_1 and u_2 are taken as an example to compare both their cost functions. According to novel cost function (16), the error vector amplitude between reference voltage vector u_{ref} and u_1 is defined as g_1, i.e., $g_1 = |u_{\text{ref}} - u_1|$, and error vector amplitude between u_{ref} and u_2 is defined as g_2, as shown in Fig. 2.

TABLE I
RELATION OF VOLTAGE VECTOR SELECTION AND SECTOR LOCATION

Sector	1	2	3	4	5	6
Vector	u_1	u_2	u_3	u_4	u_5	u_6
Vector selection	100	110	010	011	001	101

In the triangle $u_{\text{ref}} - u_1 - g_1$, the following expression can be obtained according to the cosine theorem:

$${g_1}^2 = |u_{\text{ref}}|^2 + |u_1|^2 - 2\,|u_{\text{ref}}|\,|u_1|\cos\theta_1 \tag{17}$$

where θ_1 represents the angle between u_{ref} and u_1. In the same way, the expression of the error g_2 is given by

$${g_2}^2 = |u_{\text{ref}}|^2 + |u_2|^2 - 2\,|u_{\text{ref}}|\,|u_2|\cos\theta_2 \tag{18}$$

where θ_2 represents the angle between u_{ref} and u_2. Then, subtracting (18) from (17), the square deviation between g_1^2 and g_2^2 can be calculated as follows:

$$g_1^2 - g_2^2 = |u_1|^2 - |u_2|^2 - 2\,|u_{\text{ref}}|\,(|u_1|\cos\theta_1 - |u_2|\cos\theta_2)\,. \tag{19}$$

Note that the amplitude of six nonzero vectors is equal, which means that $|u_1| = |u_2|$ and $|u_1|^2 = |u_2|^2$ are always correct. Moreover, since $\theta_1 < \theta_2$, and cosine function is monotone decreasing when angle is between 0 and 180°, (19) can be simplified as follows:

$$g_1^2 - g_2^2 = -2\,|u_{\text{ref}}|\,|u_1|\,(\cos\theta_1 - \cos\theta_2) < 0. \tag{20}$$

According to mathematical formula about difference of two squares, inequality (20) can be further simplified as follows:

$$g_1^2 - g_2^2 = (g_1 + g_2)\,(g_1 - g_2) < 0. \tag{21}$$

Inequality (21) implies that $g_1 < g_2$. This means that u_1 is better vector compared with u_2. Similarly, it can be proved that the cost function g_1 using vector u_1 is minimum compared with other cost function, which means that u_1 should be selected as optimal voltage vector (the first vector). Therefore, the first voltage vector can be easily determined according to the sector location. The relation between first vector selection and sector location is described in Table I. It is obvious that the nonzero vector selection based on sector-location can avoid all six nonzero vectors to be tested during each predictive step, which evidently reduces computation burden.

The nonzero voltage vector is first selected based on the sector location, and then the next step is to optimize the working time of nonzero vector and zero vector. First, selected nonzero voltage vector is defined as u_{opt}, and assuming that vector u_{opt} will be applied for t_{opt} and the second voltage vector, i.e., a null vector, will be applied for $T_s - t_{\text{opt}}$. It can be seen that the minimum error magnitude between reference voltage vector u^{ref} and selected nonzero vector u_{opt}, i.e., $|\Delta u_{\text{opt}}|$ shown in Fig. 3, can be obtained when vector Δu_{opt} is perpendicular to vector u_{opt}. Then, based on the vector operation, the following expression can be obtained:

$$u_{\text{ref}} \cdot u_{\text{opt}} = |u_{\text{ref}}|\,|u_{\text{opt}}|\cos\theta_{\text{opt}}. \tag{22}$$

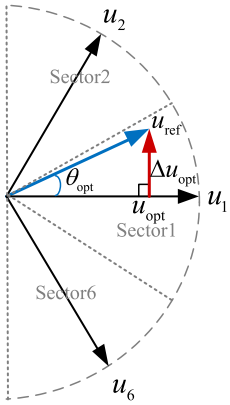

Fig. 3. Principle diagram of vector duration calculation.

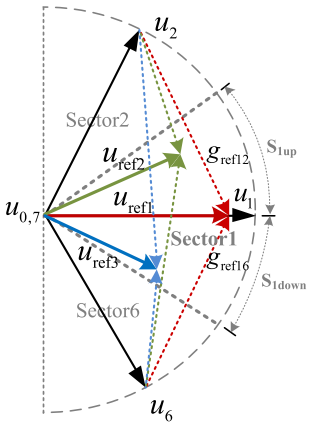

Fig. 4. Principle diagram of the second vector selection.

Moreover, according to the mathematical relation in right-angled triangle, angle $\theta_{\rm opt}$ can be expressed as follows:

$$\cos\theta_{\rm opt} = \frac{|u_{\rm opt}|\, t_{\rm opt}}{|u_{\rm ref}|\, T_{\rm s}}. \tag{23}$$

Thus, the working time of nonzero vector in one control period can be obtained as follows by substituting (23) into (22):

$$t_{\rm opt} = \frac{u_{\rm ref} \cdot u_{\rm opt}}{|u_{\rm opt}|^2} T_s. \tag{24}$$

Based on (24), the working time of null vector can easily be determined, i.e., $T_s - t_{\rm opt}$. Then, two vectors and their durations are combined as the gate signal of the inverter. In practical application, the proposed method mainly includes the following steps.

1) Measure the currents at the *k*th sampling period and compensate one step delay based on (6).
2) Predict the torque and stator flux at the (k+1)th sampling period.
3) Calculate the solution of DB-DTFC by (12) and (13), and predict reference voltage vector.
4) Calculate the sector of reference voltage vector by (14). Then, according to Table I, select nonzero voltage vectors.

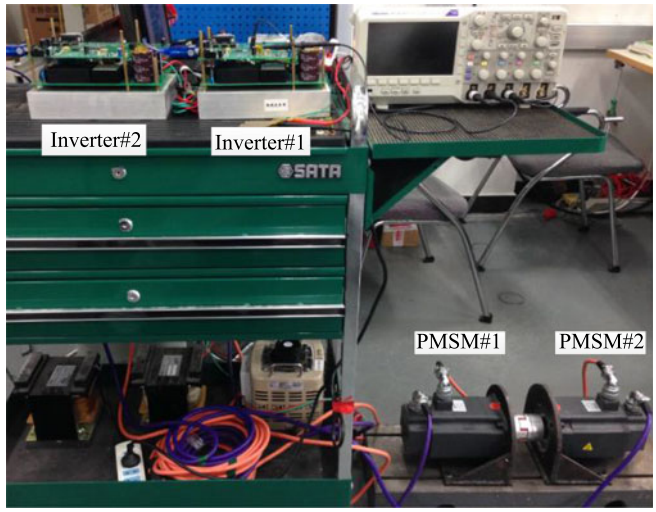

Fig. 5. Experiment platform of the PMSM system.

TABLE II
PARAMETERS OF PMSM

d- and *q*-axes inductances	$L_d = L_q = 6.183\,\text{mH}$
Stator phase resistance	$R = 3.95\,\Omega$
Rated speed	$n_N = 2000\,\text{r/min}$
Number of pole pairs	$P = 3$
Rotational inertia	$J = 0.00129\,\text{kg}\cdot\text{m}^2$
Flux linkage of permanent magnets	$\psi_a = 0.295\,\text{Wb}$

5) Calculate the working time of nonzero vector and null vector based on (24).
6) Two vectors and their durations are combined as a whole, then, apply this combined vector as the gate signal of the inverter.

IV. DVMPTC Method With One Nonzero Vector and One Unrestricted Vector

In order to further improved the steady-state performance of proposed DVMPTC with nonzero vector and one null vector, a different vector selection way, in which the second voltage vector is not fixed as a null vector but selected in a border range, is adopted in this session. The candidate vector of second voltage vector is confirmed according to the location of reference voltage vector. As the second voltage vector is also optimized in the proposed method, better control performance can be achieved.

A. Vector Selection

Similar to the DVMPTC method with nonzero vector and one null vector, the first nonzero vector $u_{1\rm opt}$ is selected based on the sector position of reference voltage vector. However, the selection way of second vector between both methods is different. Second voltage vector can be selected from null vectors or nonzero vectors, which means that the second voltage vector is not restricted to a null vector [23]. But, to avoid high switching frequency, no more than one change of switching state during one control period should be considered as the selection condition of the second voltage vector. Thus, the candidate vectors

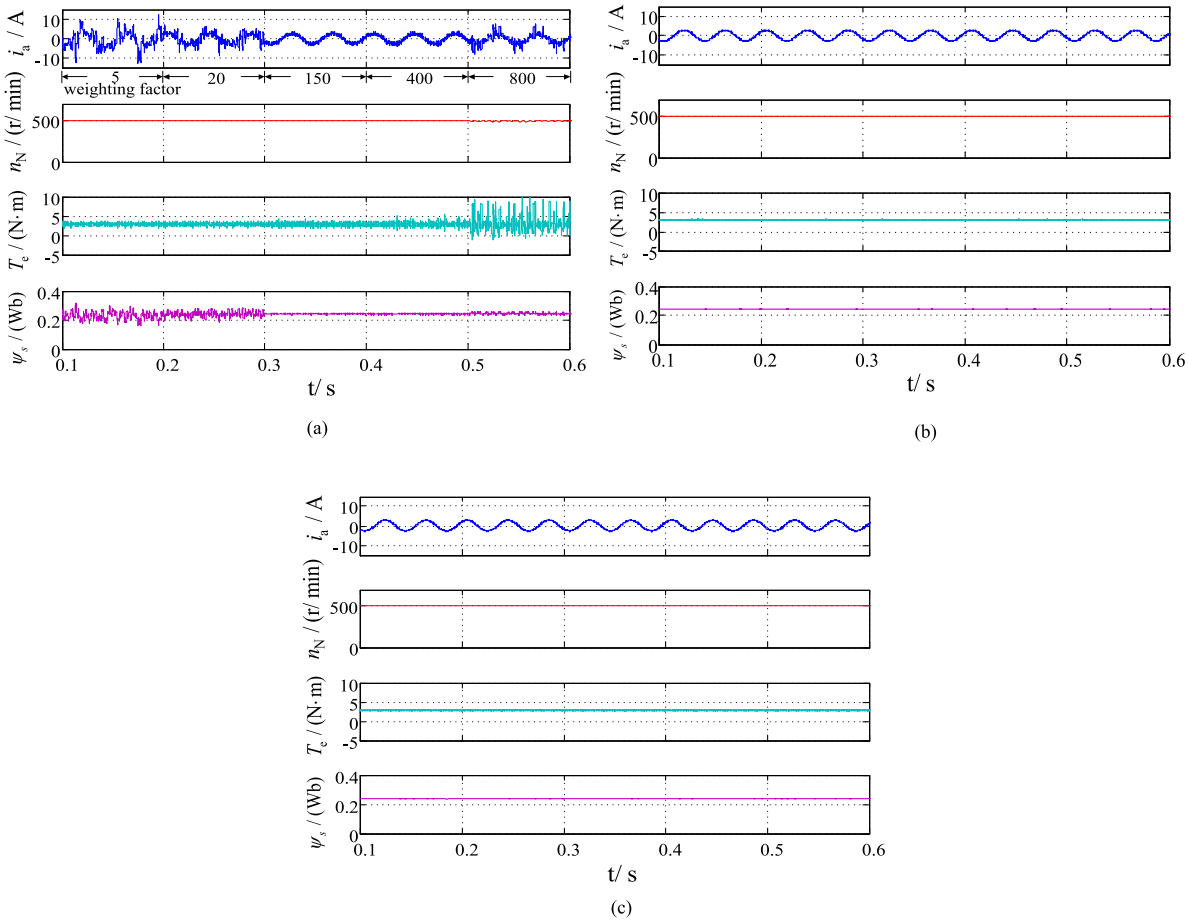

Fig. 6. Simulation results at 500 r/min with 50% rated load. (a) Two-vector-MPTC with different weighting factors. (b) Proposed MPTC I. (c) Proposed MPTC II.

of the second voltage vector can be confirmed. It means that when the first voltage vector $u_{1\mathrm{opt}}$ is determined, three voltage vectors, which include two nonzero vectors adjacent to $u_{1\mathrm{out}}$ and a null vector, can be selected as the candidate vectors of the second voltage vector. For example, if the first vector is u_i $(i = 1, 2, \ldots, 6)$, the second vector is selected from two adjacent nonzero vectors u_{i-1}, u_{i+1} and zero vector $u_{0,7}$. However, it should be note that three candidate vectors can be reduced to two based on the different sector position of reference voltage vector u_{ref}. The selection process of vector is described as follows.

1) If reference voltage vector locates the angle bisector of Section I, as shown in Fig. 4, two candidate vectors, which includes one nonzero vector u_2 or u_6 and a null vector u_0, need to be evaluated by cost function (16). Because the error vector amplitude between u_{ref1} and u_2 $(g_{\mathrm{ref12}} = |u_{\mathrm{ref1}} - u_2|)$ and error vector amplitude between u_{ref} and u_6 $(g_{\mathrm{ref16}} = |u_{\mathrm{ref1}} - u_6|)$ is equal. It means that voltage vectors u_2 and u_6 have the same control performance in this condition.
2) If reference voltage vector is in region $\mathrm{S}_{1\mathrm{up}}$ of Section I, two candidate vectors, which includes one nonzero vector u_2 and a null vector u_0, need to be evaluated by cost function (16). The nonzero vector u_6 is not required to test, because the error vector amplitude between u_{ref2} and u_2 $(g_{\mathrm{ref22}} = |u_{\mathrm{ref2}} - u_2|)$ is smaller than error vector amplitude between u_{ref2} and u_6 $(g_{\mathrm{ref26}} = |u_{\mathrm{ref2}} - u_6|)$.
3) If reference voltage vector is in region $\mathrm{S}_{1\mathrm{down}}$ of Section I, two candidate vectors, which includes one nonzero vector u_6 and a null vector u_0, need to be evaluated by cost function (16). The nonzero vector u_2 is not required to test, because the error vector amplitude between u_{ref3} and u_6 $(g_{\mathrm{ref36}} = |u_{\mathrm{ref3}} - u_6|)$ is smaller than error vector amplitude between u_{ref3} and u_2 $(g_{\mathrm{ref32}} = |u_{\mathrm{ref3}} - u_2|)$.

It can be seen that different two voltage vectors among three candidate vectors need to be evaluated by cost function, according to the sector position of u_{ref}.

B. Vector Duration Calculation

Assuming that the first voltage vector $u_{1\mathrm{opt}}$ will be applied for $t_{1\mathrm{opt}}$ and the candidate vector of the second voltage vector $u_{2\mathrm{c}}$ will be applied for $T_{\mathrm{s}} - t_{1\mathrm{opt}}$. The cost function in the quadratic form can be expressed as follows:

$$g^2 = |u_{\mathrm{ref}} - t_{1\mathrm{opt}} u_{1\mathrm{opt}} - (T_s - t_{1\mathrm{opt}}) u_{2c}|^2. \qquad (25)$$

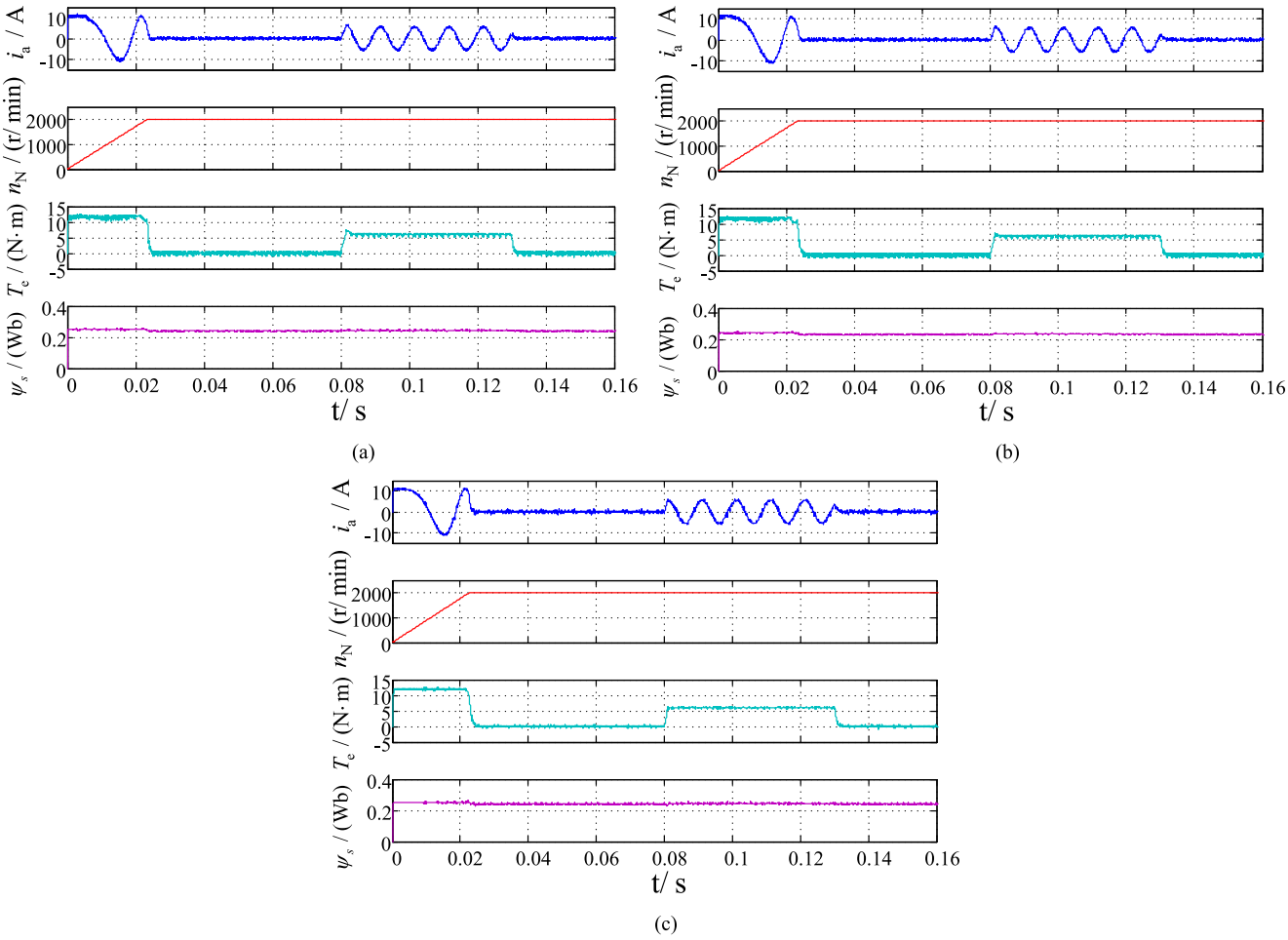

Fig. 7. Dynamic test of three methods. (a) Two-vector-MPTC. (b) Proposed MPTC I. (c) Proposed MPTC II.

TABLE III
COMPUTATION BURDEN OF CONVENTIONAL MPTC AND THE PROPOSED MPTC

Method	Conventional MPTC	Proposed MPTC-I	Proposed MPTC-II
Times (μs)	39.72	37.2	37.09
Call times of vectors	7	1	2
Time reduction (μs)	–	2.52	2.63

To obtain minimum amplitude of voltage error, the cost function g should be minimized; thus, following equation can be adopted to solve the optimal time:

$$\frac{\partial(g^2)}{\partial t_{1\mathrm{opt}}} = 0. \tag{26}$$

Thus, the optimal time $t_{1\mathrm{opt}}$ can be obtained as follows:

$$t_{1\mathrm{opt}} = \frac{(u_{\mathrm{ref}} - T_{\mathrm{s}}u_{2c}) \cdot (u_{1\mathrm{opt}} - u_{2c})}{(u_{2c} - u_{1\mathrm{opt}})^2}. \tag{27}$$

The working time of second voltage vector can easily be determined, i.e., $T_{\mathrm{s}} - t_{1\mathrm{opt}}$. After $t_{1\mathrm{opt}}$ and $T_{\mathrm{s}} - t_{1\mathrm{opt}}$ for all candidate voltage vector combinations are obtained, the cost function $g = |u_{\mathrm{ref}} - t_{1\mathrm{opt}}u_{1\mathrm{opt}} - (T_{\mathrm{s}} - t_{1\mathrm{opt}})u_{2\mathrm{c}}|$ can be calculated. Then, the optimal second voltage vector and corresponding duration producing minimal cost function would be selected.

V. SIMULATION AND EXPERIMENTAL RESULTS

In this section, to demonstrate the effectiveness of the proposed MPTC method, simulations, and experiments of prior two-vector-based MPTC [13] and the proposed two kinds of MPTC methods in one PMSM system were carried out. For simplicity, the prior method in [13] is named as two-vector-MPTC; the proposed two vectors MPTC with one nonzero vector and a null vector is named as MPTC-I and the proposed MPTC with nonzero vector and one unrestricted vector is named as MPTC-II in the following text. Simulations are established in MATLAB/Simulink. The experiments platform that is shown in Fig. 5 is constructed by TI processor and the sampling frequency is 10 kHz, and the parameters of PMSM are listed in Table II. The sample time and the PMSM parameters used in the simulation both are the same as experimental condition.

A. Simulation Results

The simulation results of two-vector-MPTC with different weighting factor are shown in Fig. 6(a). According to literature [13], the equal importance between torque and stator flux is

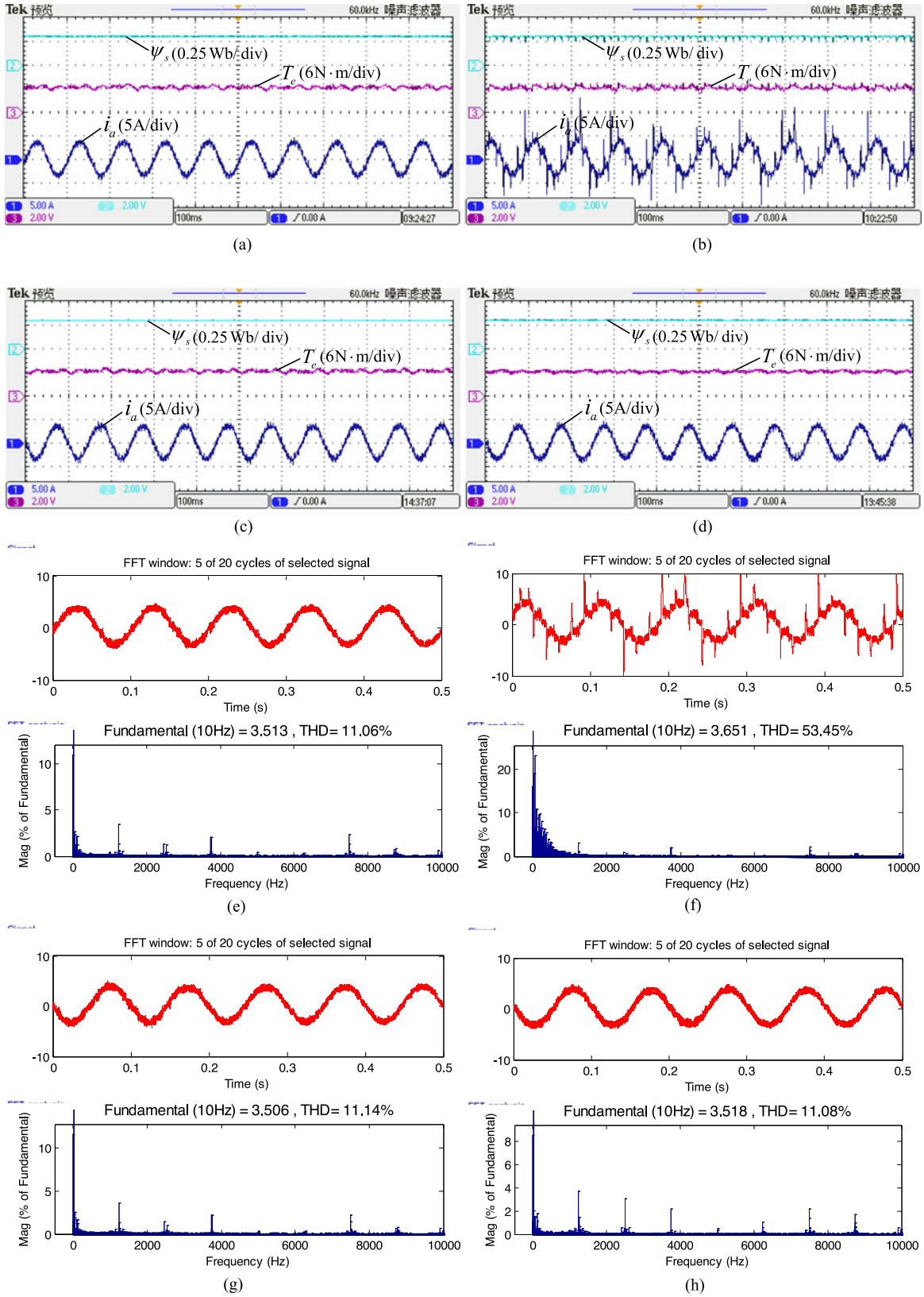

Fig. 8. Steady-state experimental results of three methods at low speed of 200 r/min and rated load. (a) Two-vector-MPTC with $A = 150$. (b) Two-vector-MPTC with $A = 20$. (c) Proposed MPTC-I. (d) Proposed MPTC-II. (e) THD analysis of two-vector-MPTC with $A = 150$. (f) THD analysis of two-vector-MPTC with $A = 20$. (g) THD analysis of the proposed MPTC-I. (h) THD analysis of the proposed MPTC-II.

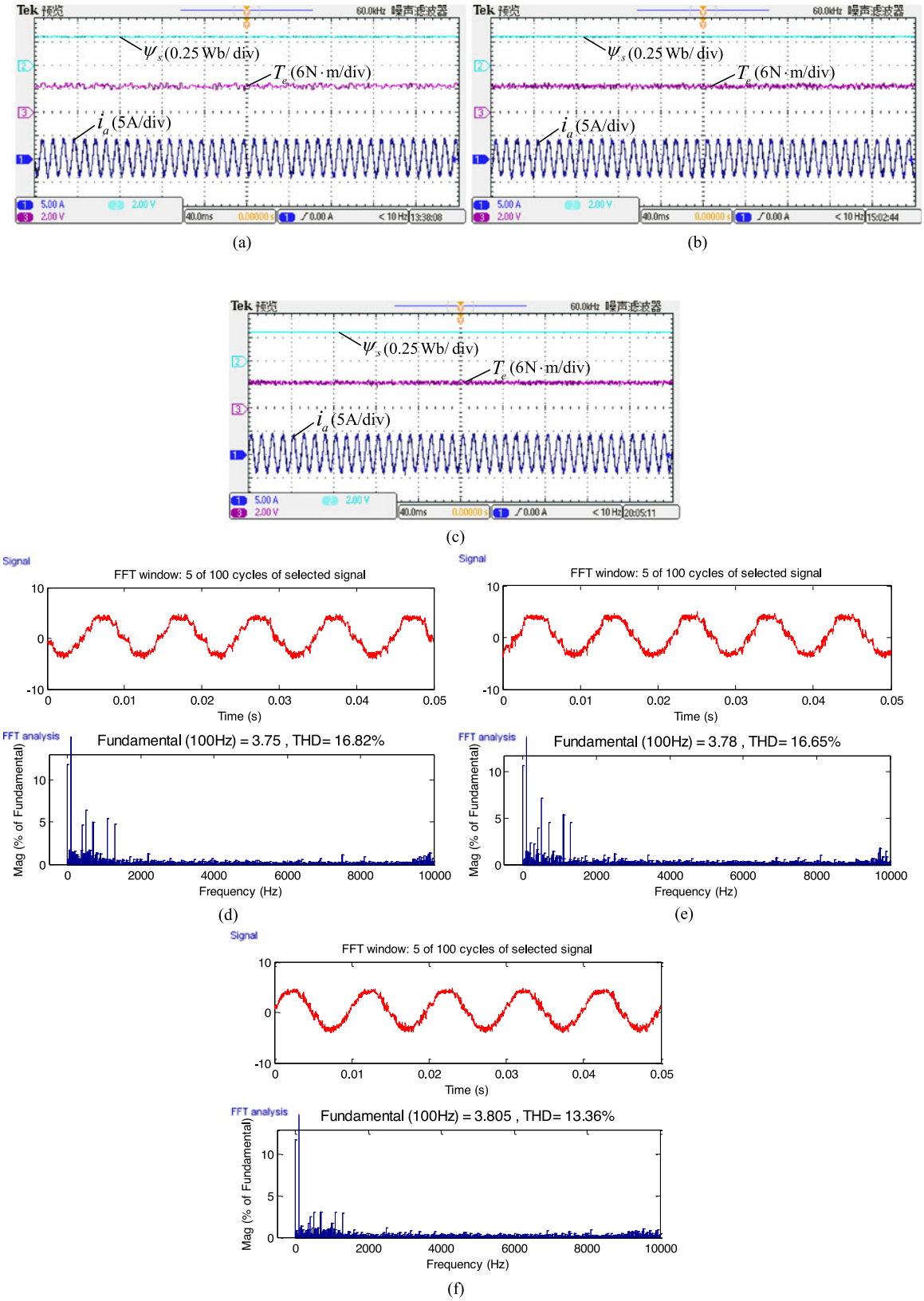

Fig. 9. Steady-state experimental results of three methods at high speed of 2000 r/min and rated load. (a) Two-vector-MPTC with optimal weighting factor. (b) Proposed MPTC-I. (c) Proposed MPTC-II. (d) THD analysis of two-vector-MPTC. (e) THD analysis of the proposed MPTC-I. (f) THD analysis of the proposed MPTC-II.

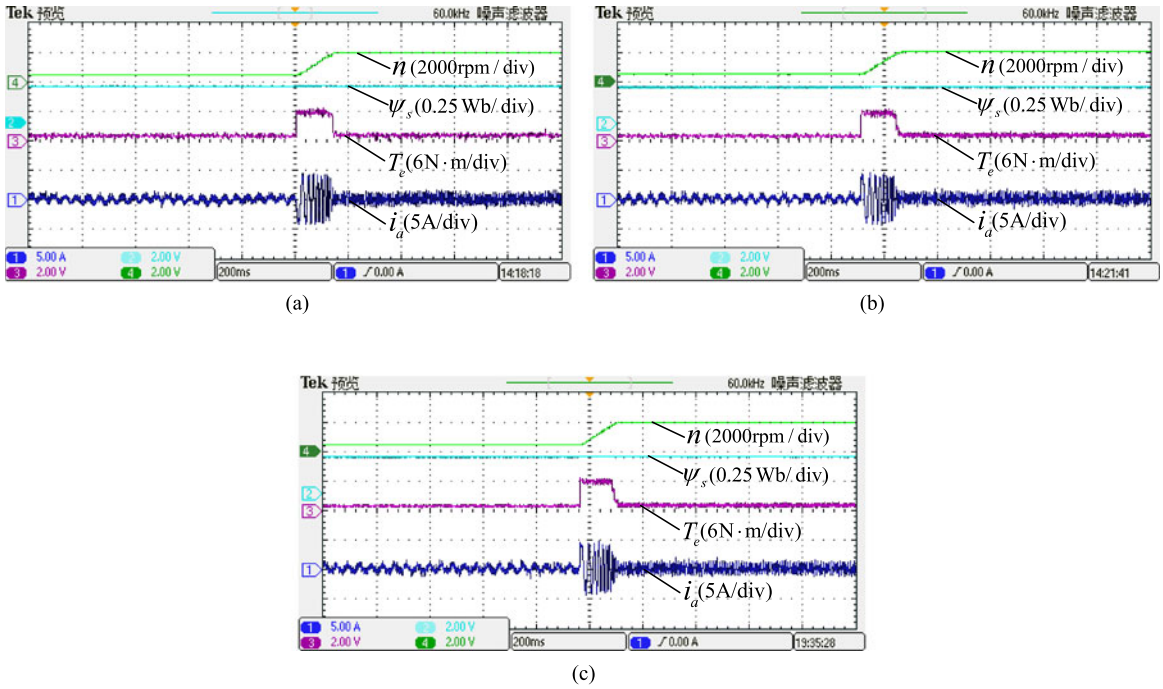

Fig. 10. Dynamic response to the variation of speed reference. (a) Two-vector-MPTC with optimal weighting factor. (b) Proposed MPTC-I. (c) Proposed MPTC-II.

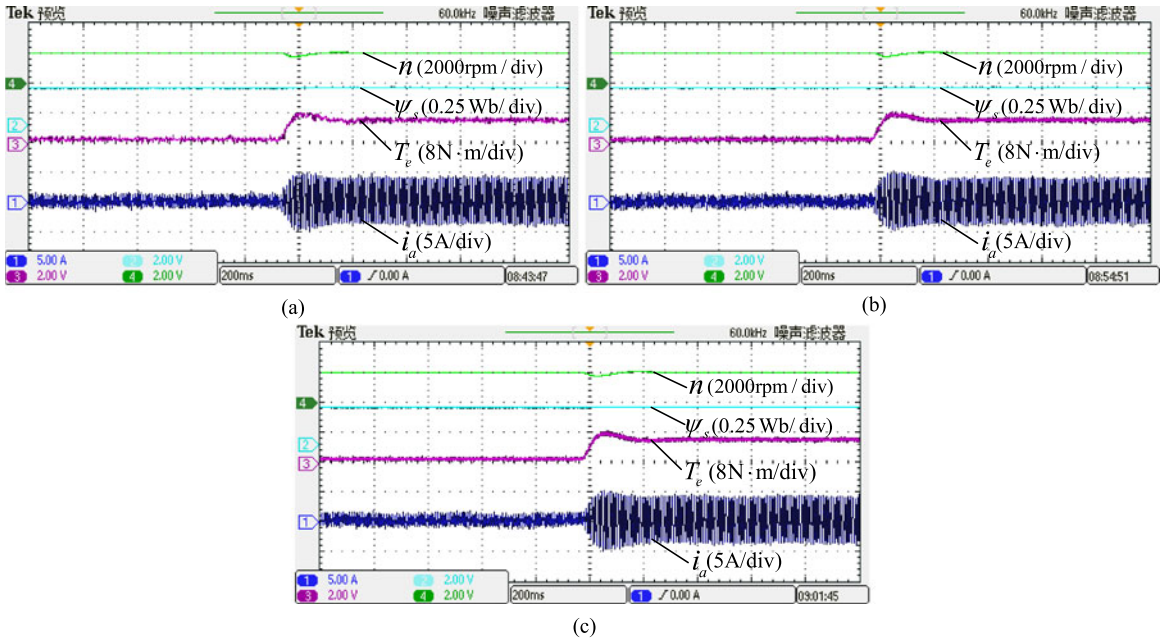

Fig. 11. Dynamic response to rated load disturbance at rated speed. (a) Two-vector-MPTC with optimal weighting factor. (b) Proposed MPTC-I. (c) Proposed MPTC-II.

considered in system control, then, the weighting factor is set as 20. However, according to the simulation results between 0.2 and 0.3 s, the control performance is not satisfactory. When the weighting factor is increased, the control performances of two-vector-MPTC become better and better. The excellent control performances are obtained when weighting factor is selected as 150. In this stage, torque and stator flux are smooth and current ripple is small. But, when the weighting factor is further increased from 150 to 800, the control performances became worse. On the other hand, when the weighting factor is reduced from 20 to 5, the control performances become very bad. It can be seen that the MPTC method is sensitive to the variation of weighting factor. Therefore, to achieve excellent control performance, lots of work is required to select a suitable weighting

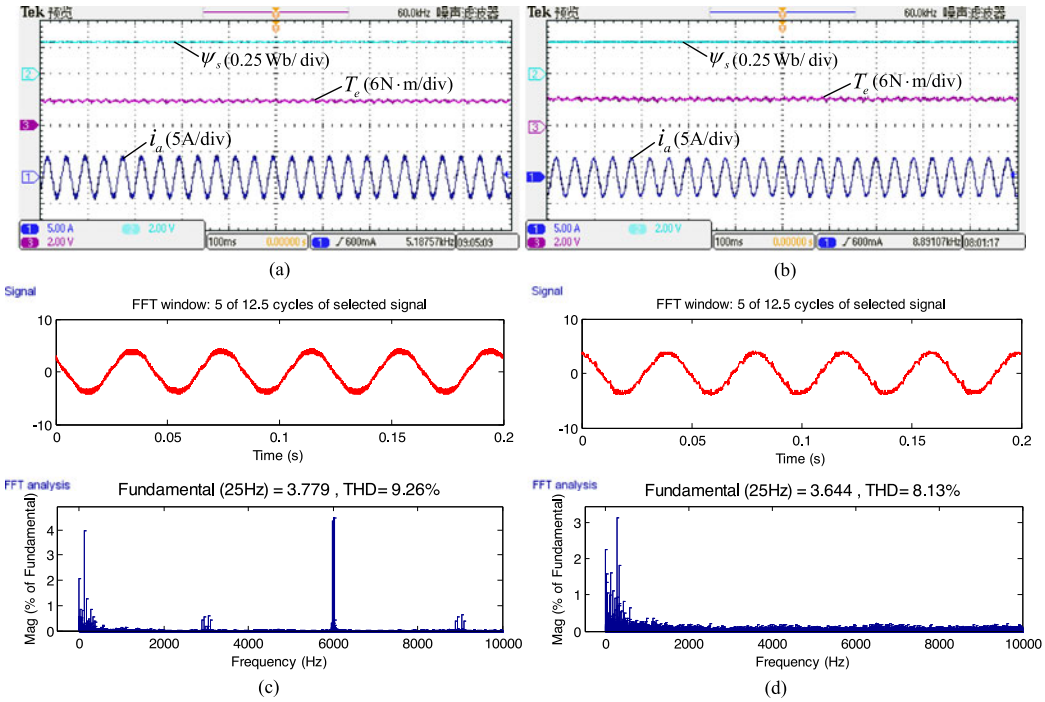

Fig. 12. Steady-state experimental results of the MPTC-II and SVM-based method at speed of 500 r/min and rated load. (a) SVM-based method. (b) Proposed MPTC-II. (c) THD analysis of the SVM-based method. (d) THD analysis of MPTC-II.

factor in the conventional method. Unlike two-vector-MPTC, the proposed MPTC methods eliminate the use of weighting factor. The control performances of the proposed MPTC-I and MPTC-II are shown in Fig. 6(b) and (c), respectively. According to results of Fig. 6(a)–(c), it is obvious that two-vector-MPTC, MPTC-I and MPTC-II have similar control performances when the optimal weighting factor is used in two-vector-MPTC. However, MPTC-I and MPTC-II avoid lots of tuning work of weighting factor, which is a advantage in the practical application.

To further evaluate the control performance of three methods, the dynamic response tests are carried out and the simulation results are compared in Fig. 7. At the start of simulation, the motor accelerates from still to rated speed 2000 r/min, and then at 0.08 and 0.13 s, rated load torque is suddenly increased and decreased, respectively. From the simulation results, it is seen that MPTC-I and MPTC-II have similar dynamic performances as two-vector-MPTC with optimal weighting factor. In other words, the proposed MPTC-I and MPTC-II not only inherit traditional advantage of MPTC, i.e., quick dynamic response, but also have their own advantage of no weighting factor.

B. Experimental Results

In order to obtain satisfactory control performance under different conditions, the weighting factor of two-vector-MPTC is tuned based on lots of experimental tests and finally it is selected as 150. The steady response at low speed $200\,\mathrm{r/min}$ with rated load under different control methods is shown in Fig. 8. Fig. 8(a) and (b) shows the performances of two-vector-MPTC with weighting factor of 150 and 20, respectively. Contrast test indicates that the weighing factor has significant influence on the control performances of the two-vector-MPTC method. When the weighting factor is reduced from 150 to 20, the torque ripple and the control performance of stator flux are deteriorated. If the weighting factor is further reduced, the control performances become worse, which may lead to instability of the control system. Therefore, to achieve desired performance of both torque and flux for MPTC, tedious tuning work of weighting factor must be finished. However, from the results of Fig. 8(c) and (d), it can be seen that proposed MPTC-I and MPTC-II can achieve satisfactory control performance without weighting factor, which prove the superiority of the proposed methods compared with two-vector-MPTC. The total harmonic distortion (THD) analysis results of different control methods are shown in Fig. 8(e)–(h).

The steady-state responses at rated speed with rated load are shown in Fig. 9. Similar to the case at low speed operation [shown in Fig. 8(a), (c), and (d)], the steady-state performance of three methods at high speed operation are similar, but the current ripples in the proposed MPTC methods are smaller, which is verified by the THD analysis results of Fig. 9(d)–(f). Experimental results indicate that the proposed MPTC methods have better steady-state control performance while avoiding the use of weighing factor. Additionally, compared with MPTC-I, the control performance of MPTC-II is better because the second voltage vector is not fixed as zero vector.

The dynamic responses of three methods are shown in Figs. 10 and 11. The responses of speed, torque, stator flux, and current is shown in Fig. 10, when speed reference suddenly changes from 500 to 2000 r/min. it can be seen that the motor accelerates quickly to rated speed without large torque fluctuation,

and achieve fast and nonovershoot speed tracking. Additionally, the dynamic tests of three methods at rated speed are carried out when the rated load is added suddenly. The results are demonstrated in Fig. 11. It can be seen that three methods can obtain extremely quick dynamic response and good disturbance rejection performance. According to the steady-state and dynamic tests, it is clearly seen that the proposed MPTC-I and MPTC-II inherit the advantage of quick torque response in conventional MPTC, while avoiding the disadvantage of use of weighting factor. Hence, the proposed MPTC methods are attractive and practical compared with conventional MPTC.

In addition, the steady performance comparison between MPTC-II and support vector machine (SVM)-based deadbeat control method is investigated in this paper. To achieve fair comparison, the SVM-based method should select the similar switching frequency to the MPTC-II method, which is considered as the common practice and standard when comparing different control methods, as shown in [23] and [25]. Therefore, in order to attain similar average switching frequency of 2.97 kHz at speed of 500 r/min, the switching frequency of the SVM-based method is configured as 2.97 kHz in this paper. The steady performances of both methods are shown in Fig. 12. It can be seen that the current THD of the proposed MPTC-II is 8.13%, which is smaller than 9.26% of the SVM-based method. It means that, under the condition of the same average switching frequency, the steady performance of the MPTC-II method is better compared with the SVM-based control method.

Finally, the computation burden comparison of three methods is given by Table III. The conventional two-vector-MPTC method requires 39.72 μs to complete code operation; however, the proposed MPTC-I and MPTC-II requires 37.2 and 37.09 μs, respectively. It means that the computation burden is reduced by up to 6.34% and 6.62% by using the proposed MPTC methods.

In summary, the simulation and experimental results prove that the proposed MPTC-I and MPTC-II not only can reduce computation burden but also avoid the use of weighting factor. Therefore, the proposed MPTC methods are more practical compared with the conventional MPTC.

VI. Conclusion

In this paper, a novel two-vector-based MPTC method is proposed and has been experimentally applied to a PMSM system. The major contributions of this work include: 1) the DB-DTFC solution is introduced to select the optimal vector, then the computation time of the MPTC method is significantly reduced, which improves the practicality of two-vector-based MPTC; and 2) a novel cost function, which directly compares the reference voltage vector and candidate voltage vector, is proposed to eliminate the weighting factor, then nontrivial tuning work of weighting factor caused by indirect-voltage-selection-based cost function is avoided.

References

[1] T. Geyer, G. Papafotiou, and M. Morari, "Model predictive direct torque Control–Part I: Concept, algorithm, and analysis," *IEEE Trans. Ind. Electron.*, vol. 56, no. 6, pp. 1894–1905, Jun. 2009.

[2] G. S. Buja and M. P. Kazmierkowski, "Direct torque control of PWM inverter-fed AC motors—A survey," *IEEE Trans. Ind. Electron.*, vol. 51, no. 4, pp. 744–757, Aug. 2004.

[3] W. Xie *et al.*, "Finite-control-set model predictive torque control with a deadbeat solution for PMSM drives," *IEEE Trans. Ind. Electron.*, vol. 62, no. 9, pp. 5402–5410, Sep. 2015.

[4] Z. Xiang, X. Zhu, L. Quan, Y. Du, C. Zhang, and D. Fan, "Multi-level design optimization and operation of a brushless double mechanical ports flux-switching permanent magnet motor," *IEEE Trans. Ind. Electron.*, vol. 63, no. 10, pp. 6042–6054, Oct. 2016.

[5] J. Rodriguez and P. Cortes, *Predictive Control of Power Converters and Electrical Drives*. New York, NY, USA: Wiley, 2012.

[6] V. Yaramasu, M. Rivera, B. Wu, and J. Rodriguez, "Model predictive current control of two-level four-leg inverters—Part I: Concept, algorithm, and simulation analysis," *IEEE Trans. Power Electron.*, vol. 28, no. 7, pp. 3459–3468, Jul. 2013.

[7] W. Xie, X. Wang, F. Wang, W. Xu, R. Kennel, and D. Gerling, "Dynamic loss minimization of finite control set-model predictive torque control for electric drive system," *IEEE Trans. Power Electron.*, vol. 31, no. 1, pp. 849–860, Jan. 2016.

[8] M. Preindl and S. Bolognani, "Model predictive direct speed control with finite control set of PMSM drive systems," *IEEE Trans. Power Electron.*, vol. 28, no. 2, pp. 1007–1015, Feb. 2013.

[9] S. A. Davari, D. A. Khaburi, and R. Kennel, "An improved FCS-MPC algorithm for an induction motor with an imposed optimized weighting factor," *IEEE Trans. Power Electron.*, vol. 27, no. 3, pp. 1540–1551, Mar. 2012.

[10] F. Villarroel *et al.*, "Multiobjective switching state selector for finite states model predictive control based on fuzzy decision making in a matrix converter," *IEEE Trans. Ind. Electron.*, vol. 60, no. 2, pp. 589–599, Feb. 2013.

[11] C. A. Rojas, J. Rodriguez, F. Villarroel, J. R. Espinoza, C. A. Silva, and M. Trincado, "Predictive torque and flux control without weighting factors," *IEEE Trans. Ind. Electron.*, vol. 60, no. 2, pp. 681–690, Feb. 2013.

[12] P. Cortes *et al.*, "Guidelines for weighting factors design in model predictive control of power converters and drives," in *Proc. IEEE Int. Conf. Ind. Technol.*, 2009, pp. 1–7.

[13] Y. Zhang and H. Yang, "Model predictive torque control of induction motor drives with optimal duty cycle control," *IEEE Trans. Power Electron.*, vol. 29, no. 12, pp. 6593–6603, Dec. 2014.

[14] D. Casadei, F. Profumo, G. Serra, and A. Tani, "FOC and DTC: Two viable schemes for induction motors torque control," *IEEE Trans. Power Electron.*, vol. 17, no. 5, pp. 779–787, Sep. 2002.

[15] G. Foo and M. F. Rahman, "Sensorless direct torque and flux-controlled IPM synchronous motor drive at very low speed without signal injection," *IEEE Trans. Ind. Electron.*, vol. 57, no. 1, pp. 395–403, Jan. 2010.

[16] T. Geyer and D. E. Quevedo, "Performance of multistep finite control set model predictive control for power electronics," *IEEE Trans. Power Electron.*, vol. 30, no. 3, pp. 1633–1644, Mar. 2015.

[17] T. Geyer and D. E. Quevedo, "Multistep finite control set model predictive control for power electronics," *IEEE Trans. Power Electron.*, vol. 29, no. 12, pp. 6836–6846, Dec. 2014.

[18] A. Linder and R. Kennel, "Model predictive control for electrical drives," in *Proc. IEEE 36th Power Electron. Spec. Conf.*, Jun. 2005, pp. 1793–1799.

[19] P. Stolze, M. Tomlinson, R. Kennel, and T. Mouton, "Heuristic finite-set model predictive current control for induction machines," in *Proc. IEEE Energy Convers. Congr. Expo. Asia*, Downunder, Jun. 2013, pp. 1221–1226.

[20] M. Nemec, D. Nedeljkovic, and V. Ambrozic, "Predictive torque control of induction machines using immediate flux control," *IEEE Trans. Ind. Electron.*, vol. 54, no. 4, pp. 2009–2017, Aug. 2007.

[21] Y. Shi, K. Sun, L. Huang, and Y. Li, "Online identification of permanent magnet flux based on extended Kalman filter for IPMSM drive with position sensorless control," *IEEE Trans. Ind. Electron.*, vol. 59, no. 11, pp. 4169–4178, Nov. 2012.

[22] Y. C. Zhang, W. Xie, and Z. X. Li, "Low-complexity model predictive power control: Double-vector-based approach," *IEEE Trans. Ind. Electron.*, vol. 61, no. 11, pp. 5871–5880, Nov. 2014.

[23] Y. C. Zhang, Y. B. Peng, and H. T. Yang, "Performance improvement of two-vector-based model predictive control of PWM rectifier," *IEEE Trans. Power Electron.*, vol. 31, no. 8, pp. 6016–6030, Aug. 2016.

[24] Y. Zhang and H. Yang, "Model-predictive flux control of induction motor drives with switching instant optimization," *IEEE Trans. Energy Convers.*, vol. 33, no. 3, pp. 1113–1122, Sep. 2015.

[25] F. Morel, X. Lin-Shi, J.-M. Retif, B. Allard, and C. Buttay, "A comparative study of predictive current control schemes for a permanent-magnet synchronous machine drive," *IEEE Trans. Ind. Electron.*, vol. 56, no. 7, pp. 2715–2728, Jul. 2009.

Xiaoguang Zhang (M'15) received the B.S. degree from Heilongjiang Institute of Technology, Harbin, China, in 2007, and the M.S. and Ph.D. degrees from Harbin Institute of Technology, Harbin, in 2009 and 2014, respectively, all in electrical engineering.

He is currently an Assistant Professor at the North China University of Technology, Beijing, China. From 2012 to 2013, he was a Research Associate with Wisconsin Electric Machines and Power Electronics Consortium, University of Wisconsin–Madison, Madison. His research interests include power electronics and electric machines drives.

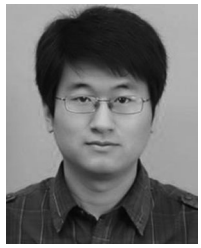

Benshuai Hou was born in Shandong, China, in 1989. He received the B.S. degree in electrical engineering from Beijing Union University, Beijing, China, in 2013, and is currently working toward the M.S. degree at the North China University of Technology, Beijing.

His research interests include permanent magnet machines and drives.